Loop-extruders alter bacterial chromosome topology to direct entropic forces for segregation

Janni Harju[1], **Muriel C. F. van Teeseling**[2], **and Chase P. Broedersz**[1,3,✉]

[1]Department of Physics and Astronomy, Vrije Universiteit Amsterdam, 1081 HV Amsterdam, The Netherlands
[2]Junior research group Prokaryotic Cell Biology, Department Microbial Interactions, Institute of Microbiology, Friedrich-Schiller-Universität, Jena, Germany
[3]Arnold Sommerfeld Center for Theoretical Physics and Center for NanoScience, Department of Physics, Ludwig-Maximilian-University Munich, Theresienstr. 37, D-80333 Munich, Germany

Entropic forces have been argued to drive bacterial chromosome segregation during replication. In many bacterial species, however, specifically evolved mechanisms, such as loop-extruding SMC complexes and the ParAB*S* origin segregation system, contribute to or are even required for chromosome segregation, suggesting that entropic forces alone may be insufficient. The interplay between and the relative contributions of these segregation mechanisms remain unclear. Here, we develop a biophysical model showing that purely entropic forces actually inhibit bacterial chromosome segregation until late replication stages. By contrast, our model reveals that loop-extruders loaded at the origins of replication, as observed in many bacterial species, alter the effective topology of the chromosome, thereby redirecting and enhancing entropic forces to enable accurate chromosome segregation during replication. We confirm our model predictions with polymer simulations: purely entropic forces do not allow for concurrent replication and segregation, whereas entropic forces steered by specifically loaded loop-extruders lead to robust, global chromosome segregation during replication. Finally, we show how loop-extruders can complement locally acting origin separation mechanisms, such as the ParAB*S* system. Together, our results illustrate how changes in the geometry and topology of the polymer, induced by DNA-replication and loop-extrusion, impact the organization and segregation of bacterial chromosomes.

Correspondence: *c.p.broedersz @vu.nl*

DRAFT

Introduction

Many bacteria contain a single circular chromosome that is simultaneously replicated and segregated during the cell cycle (1–3). The physical segregation of these large DNA polymers ($\sim$ 1 mm) must be achieved rapidly, accurately, robustly, and within the tight confinement of the cell ($\sim$ 1 µm), to ensure the viability of daughter cells. Various mechanisms, including entropic forces (4), loop-extruding Structural Maintenance of Chromosomes (SMC) complexes (5–8), and the origin segregating ParAB*S* system (9–11), are implicated in the bacterial chromosome segregation process. However, the interplay between and the relative importance of these mechanisms are not fully understood. In this study, we investigate when in the replication cycle, where along the chromosome, and how these different components can individually and collectively contribute to bacterial chromosome segregation.

The concept of entropic segregation forces arises from the field of polymer physics. Put simply, two spatially confined polymers with excluded volume interactions will segregate because there are more configurations that they can adopt when they do not overlap (4, 12, 13); segregated states are more numerous and therefore have higher entropy. Entropic forces can also cause chromosomal loops to segregate, which has been proposed to affect the organization and segregation of eukaryotic (14) and prokaryotic (15) chromosomes. Previous work has suggested that entropic segregation forces could largely explain bacterial chromosome segregation (4, 16). These works theoretically focused on the entropic segregation of two fully replicated chromosomes, whereas *in vivo*, segregation is concurrent with replication (17, 18). A concentric-shell model was needed to achieve concurrent chromosome replication and segregation in simulations; a newly replicated chromosomal strand was given a larger accessible volume, an assumption that may not hold for all bacteria (16). A later simulation study showed that entropic segregation can occur when chromosomal regions corresponding to *E. coli* Macrodomains are geometrically constrained (19). Hence, while the theoretical concept of entropic segregation has gained traction, the role and importance of entropic segregation forces are still subjects of debate. When in the replication cycle are entropic segregation forces effective? And how do they act in conjunction with dedicated chromosome segregation mechanisms?

Three widely spread biological mechanisms are known to contribute to chromosome segregation in prokaryotes: loop-extrusion by SMC complexes (8, 20, 21), terminus segregation by the translocase FtsK (22–25), and origin segregation by the ParAB*S* system (26). Loop-extrusion is said to "individualize" newly replicated chromosomes, but it remains unclear how this biophysically promotes spatial segregation (3). FtsK "pumps" replicated terminal regions in opposite directions right before cell division (27, 28). Finally, at least in the model organism *Caulobacter crescentus*, the ParAB*S* system can be modeled as a locally acting force that tethers one origin of replication to a pole, and pulls the other origin to the opposite pole (29–33). In *C. crescentus*, the ParAB*S* system and FtsK are essential for chromosome segregation (11, 25) whereas the SMC condensin does not appear to be required (34–36). By contrast, *Escherichia coli* has no ParAB*S* system, and instead relies on loop-extrusion and FtsK for faithful chromosome segregation (5, 22, 37). Finally, in *Bacillus subtilis*, the ParAB*S* system and FtsK only become critical for chromosome segregation in the absence of condensin (38–40). These observations suggest that biological mechanisms can play important but sometimes over-

lapping roles during bacterial chromosome segregation. The relative contributions of these mechanisms to chromosome segregation in various species, as well as their interplay with entropic forces, remain unclear.

Here, we start by revisiting the theoretical question of whether entropic forces alone can segregate bacterial chromosomes. We develop a biophysical model and simulations for entropic segregation that take the geometry and topology of a replicating chromosome into account. We show that, until late replication stages, purely entropic forces cause the alignment of replicated chromosome strands, and therefore actually inhibit chromosome segregation. Remarkably however, our results also demonstrate that topological constraints due to origin-proximally loaded loop-extruders transform these segregation-inhibiting entropic forces into "topo-entropic" forces that efficiently drive global chromosome segregation. By contrast, we find that locally acting ParAB*S*-like separating forces alone can be insufficient to segregate terminal regions. This suggests that faithful ParAB*S*-based chromosome segregation requires either loop-extrusion or an additional dedicated terminus-segregation mechanism. Our work explains results from existing knock-out experiments, makes novel, testable predictions, and provides a conceptual framework for understanding how different bacterial chromosome segregation mechanisms operate in unison.

Results

Topo-entropic segregation model. We develop a biophysical model to gain physical intuition for how entropic forces act on the global organization of a replicating bacterial chromosome. In contrast to previous theoretical work (4), we consider how the extent of replication affects the geometry and topology of the chromosome and thereby the direction of entropic forces. For simplicity, we do not include structural features such as Chromosome Interaction Domains (CIDs) (35) or *E. coli* Macrodomains (19), nor do we assume constraints on the replication fork positions (4, 41). Using this topo-entropic segregation model, we investigate how entropic forces are affected by loop-extruders that are loaded at the origins of replication (*ori*) and traverse along the chromosomal arms towards the terminus (*ter*), as observed in multiple bacterial species.

Entropy does not segregate partially replicated circular chromosomes. To describe the global organization of a replicating chromosome, we can employ a coarse-grained polymer model. In this model, the chromosome is represented as a circular polymer with N coarse-grained monomers of length b – set to be larger than the persistence length of DNA – at a time point where R monomers have been replicated. This partially replicated chromosome exhibits excluded volume interactions and is confined to a cylinder of diameter d and length L, representing the nucleoid. Chromosomes are highly compressed: without confinement, they expand drastically (44–46). In this highly compressed limit ($Nb^{1/\nu} \gg L^{1/\nu}$, where ν is the Flory exponent), we can describe chromosomal strands as compressed entropic springs (Fig. 1A,B).

To find the entropically preferred chromosome configuration at a given replication stage, we first decompose the chromosome into the largest possible ring and a remaining linear segment connecting the replication forks (Fig. 1C). In the first half of the replication cycle ($R < N/2$), the largest ring is given by a union of one replicated strand and the unreplicated strand of the chromosome, together of length N. Once more than half of the chromosome has been replicated ($R > N/2$), the largest ring is given by the union of the two replicated strands, together of length $2R$. We seek long-axis configurations that maximize the entropies of the ring and the linear segment, under the constraint that they are conjoint at the two replication forks. To simplify our reasoning, we neglect excluded volume interactions between the ring and the linear segment, as we can use a blob scaling analysis to show that including these interactions does not change the entropically favored configuration of the chromosome (Supplementary Note 1, Supplementary Fig. 1).

The configurational entropy of the largest ring is optimized when it maximally extends across the length L of the nucleoid. But, the ring by itself has no preferred orientation; the ring can freely rotate into a different orientation. We note that including ParAB*S*-like forces, polymer structures such as Macrodomains (19) or fixed loops (15) could break this rotational symmetry. However, even in the absence of such effects, the remaining linear segment of the partially replicated chromosome breaks this symmetry and determines the entropically preferred orientation of the chromosome.

In the first half of the replication cycle, once the newly replicated linear segment is long enough to be compressed ($R \gg (d/b)^{1/\nu}$), the linear segment entropically prefers to orient and extend along the long-axis of the cell. The replication forks are hence pushed apart, resulting in a "fork-segregated", left-*ori*-right configuration, where the newly replicated chromosome segments lie parallel to each other (Fig. 1D, first cell). For the first half of the cell cycle, purely entropic forces thus inhibit chromosome segregation.

In the second half of the replication cycle, as long as the unreplicated linear segment is long enough to be compressed ($N - R \gg (d/b)^{1/\nu}$), the linear segment's entropy is again larger when the replication forks are pushed apart along the long-axis of the cell. The chromosome hence still favors a fork-segregated orientation (Fig 1D, second cell). Once replication is nearly complete ($N - R \lesssim (d/b)^{1/\nu}$), however, the limit of two conjoined circular chromosomes is reached. The unreplicated linear segment is now so short that it no longer gains entropy by aligning with the long axis, and thus no longer pushes the replication forks apart. This results in an *ori-ter-ori* configuration, and we finally achieve entropic segregation of sister chromosomes along the long-axis of the cell, as previously argued (4) (Fig 1D, third cell).

Loop-extrusion redirects entropic forces enabling segregation during replication . We next consider the effect of bidirectional loop-extruders primarily loaded at the origins of replication, such as condensin in *B. subtilis* (8, 47), *Streptococcus pneumoniae* (48), or *C. crescentus* (49). Im-

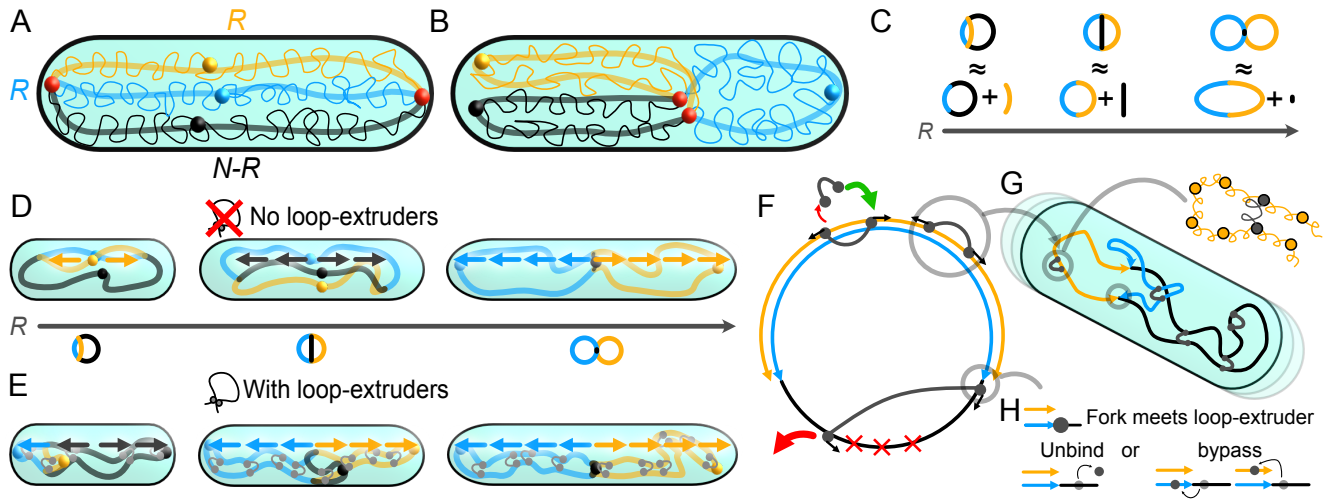

Fig. 1. Schematics for topo-entropic segregation model and simulations **A** A highly compressed circular chromosome of N monomers, with R monomers replicated, confined to a cylinder. Orange and blue lines depict newly replicated chromosomal strands, black line the unreplicated strand. In schematics, we depict only the orientation of each strand (thick lines), rather than the microscopic configuration of the highly compressed polymers (thin wiggly lines). Filled circles mark *ori*s (blue and orange), replication forks (red) and the *ter* (black). **B** Similar to A, but showing a sister strand-segregated configuration. **C** At each replication stage, we decompose the partially replicated chromosome into the largest possible ring and a linear segment. **D** The entropically favored global orientation for three distinct replication stages. Colored arrows indicate the direction of purely entropic forces. Until late replication stages, we expect fork-segregated left-*ori*-right configurations, and at late replication stages, a segregated *ori-ter-ori* configuration. **E** When loop-extruders are loaded at *ori*s, the opposite arms of the chromosome are effectively tied together. The entropically favored global configurations under these topological constraints are sketched at three replication stages. Overlaid arrows indicate the direction of topo-entropic forces. For $R < N/2$, we expect an *ori-ori-ter* configuration, and for $R \geq N/2$, a segregated *ori-ter-ori* configuration. **F** Bidirectional loop-extrusion is simulated in 1D (42, 43) on a replicating circular chromosome. The replication forks proceed independently, creating new sites where loop-extruders can move. Loop-extruders are preferably loaded at the *ori*s. The terminal region has an enhanced offloading rate. **G** Loop-extruder and replication fork positions from the 1D simulations are used to constrain 3D bead-spring polymer simulations, where loop-extruders act as springs between monomers. The replicating polymer is confined to an exponentially growing cylinder. **H** When a replication fork encounters a loop-extruder leg, the loop-extruder either unbinds or steps onto either strand on the other side of the fork.

portantly, the loop-extruders tie the opposite arms of the chromosome together, effectively changing the chromosome topology. This implies that, in the presence of enough loop-extruders, the largest chromosomal ring at a given replication stage is (at least partially) linearized, with loop-extruder loading sites acting as "chain ends". This linearized segment entropically prefers to extend across the long-axis of the cell, so that the loop-extruder loading site is near a cell pole. The region near the other origin of replication is also linearized. For the first half of the replication cycle, the preferred chromosome configuration is then *ori-ori-ter* (Fig. 1E, first cell), and for the second half, *ori-ter-ori* (Fig. 1E, second and third cell). A blob scaling argument shows that loop-extruders loaded at the origins also shift the free energy due to chain overlap in favor of the global orientations sketched in Fig. 1E (Supplementary Note 2, Supplementary Fig. 1). Conceptually, the entropic forces are modified by topological constraints on the polymer imposed by loop-extruders, into "topo-entropic" forces. In contrast to purely entropic forces, topo-entropic forces drive chromosome segregation concurrent with replication.

In summary, by developing this topo-entropic segregation model that takes into account the geometry and topology of a replicating chromosome, we reason that, unlike previously proposed (4), entropic forces inhibit rather than promote bacterial chromosome segregation for most of the replication cycle. Importantly, we also find that concurrent replication and segregation can be recovered if loop-extruders redirect entropic forces by changing the effective topology of the chromosome.

Simulations of a replicating chromosome. To test our predictions, we construct a computational model for loop-extrusion on a replicating bacterial chromosome, by adapting a previously published algorithm for a single bacterial chromosome (42, 43), with system parameters based on experimental data (42, 43, 50–53) (Supplementary Notes 3-4). Briefly, we first simulate the movements of a set of loop-extruders and two independently moving replication forks on a 1D lattice (Fig. 1F). When a loop-extruder leg encounters a replication fork, it either unbinds with a probability P_{U}, or steps to either DNA strand on the other side of the fork with equal probabilities (Fig. 1H). Similar rules are defined for cases where loop-extruders overtake replication forks (Supplementary Fig. 2). We find that increasing P_{U} slightly improves segregation, but does not qualitatively impact our results (Supplementary Fig. 3), and hence use a value of $P_{\mathrm{U}} = 0$ unless otherwise stated. The loop-extruder and fork positions from the 1D simulations are then imposed as moving constraints in molecular dynamics simulations of a 3D polymer (Fig. 1G). These coarse-grained simulations have sufficiently strong excluded volume effects that the polymer exhibits self-avoiding behavior (Supplementary Note 5, Supplementary Fig. 4). Finally, the replicating chromosome is confined to an exponentially growing cylinder to model cell growth, and we can add origin-pulling forces to qualitatively model the ParAB*S* system (Supplementary Note 6). This computational model allows us to test how different mechanisms (individually and together) affect the spatio-temporal organization of replicating chromosomes.

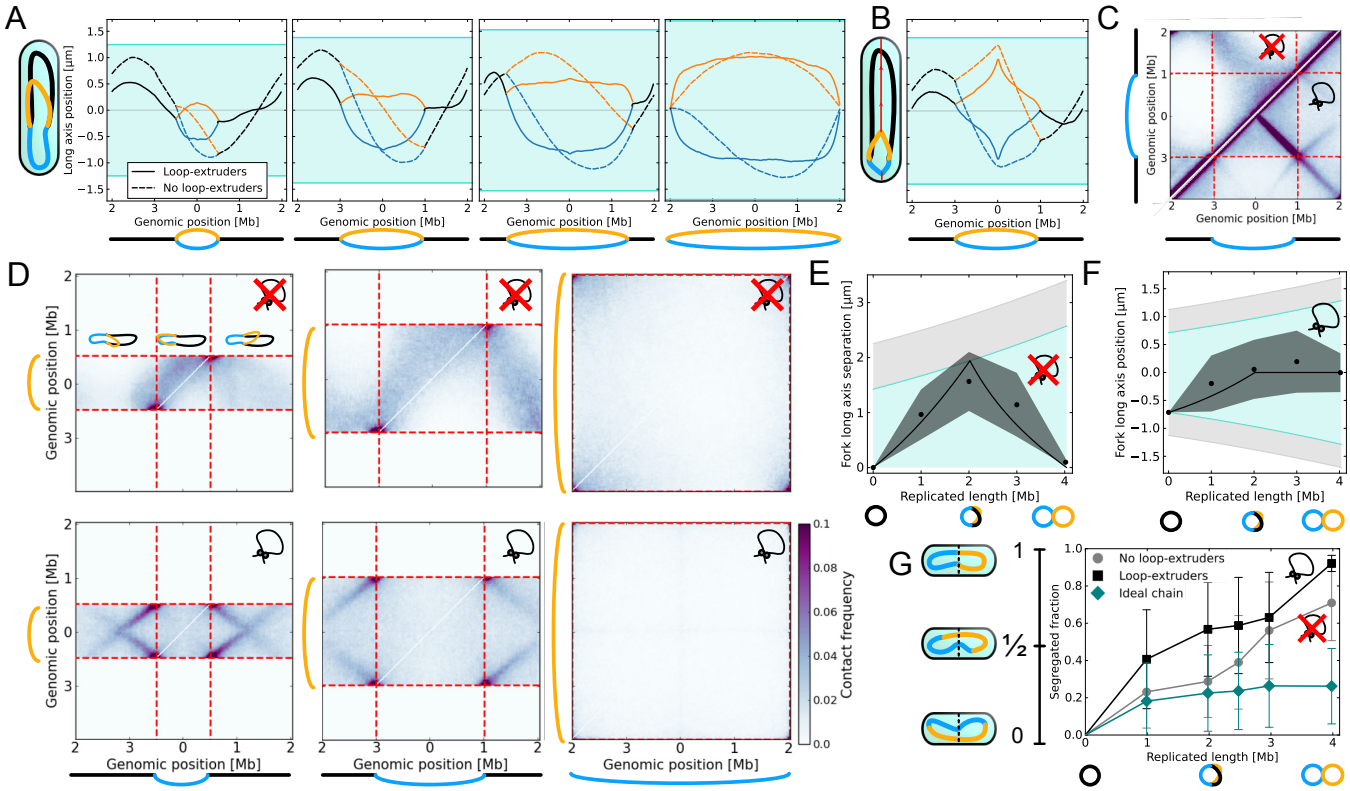

Fig. 2. Steady-state simulations of chromosome organization at different replication stages Icons with (crossed) loops indicate whether simulations were conducted with (without) loop-extruders. **A** Steady-state mean long-axis positions loci as a function of genomic position for $R = 100, 200, 300$, or 402. Total chromosome length $N = 404$. Without loop-extruders, replication forks separate, whereas with loop-extruders, they occupy the same mean long-axis position. **B** When *ori*-pulling forces are added, steady-state configurations without loop-extruders still exhibit fork segregation. With loop-extrusion, regions near the forks are better segregated. Data for $R = 200$, Supplementary Fig. 9 shows other replication stages. **C** Intrachromosomal contact maps at $R = 200$. Without loop-extruders (top-left), the chromosome folds from mid-arm, consistent with a fork-segregated left-*ori*-right configuration. With loop-extruders (bottom-right), the chromosome folds from the *ori*, consistent with an *ori-ter* organization. Weaker lines from the replication forks arise from the unreplicated segment folding towards the origin of replication. Color bar in Subfigure D. **D** Inter-chromosomal contact maps for $R = 100, 200, 402$. Without loop-extruders (top row), inter-chromosomal contacts only diminish when $R \approx N$. With loop-extrusion (bottom row), inter-chromosomal contacts are diminished earlier. Inset in top-left contact map illustrates chromosome configurations that would give contacts for each section of the map. **E** Mean steady-state long-axis separation between replication forks without loop-extruders. Black line gives a prediction calculated by assuming that the distance between the forks scales with the shortest genomic length between them (Supplementary Note 7). Turquoise indicates estimated maximum separation, light-gray indicates confinement length L. **F** Mean steady-state long-axis position of replication forks with loop-extruders. The distance between *ori* 1 and the replication forks is predicted to scale with $R/2$ for $R < N/2$, after which the forks should stay at mid-cell. **G** Segregated fraction as a function of replicated length for simulations with loop-extruders, without loop-extruders, and an ideal chain without loop-extruders. Error bars indicate standard deviation.

Loop-extruders prevent entropically favored fork segregation. The efficiency of chromosome segregation depends on two factors: the directions of the relevant forces, which determine the steady-state configuration a partially replicated chromosome would relax to given enough time, and the speed at which the system relaxes. To test our predictions for the directions of entropic forces and the resulting global organization with and without loop-extrusion, we start by investigating steady-state simulations with a given, fixed replicated length R. We initialize simulations with unsegregated, overlapping *ori-ter* configurations. Simulations are run long enough that the mean long-axis positions of various loci converge to steady-state values (Supplementary Fig. 5). Since the two replicated strands are identical, averaging over sampled configurations yields the same statistics for both replicated strands, as well as for both replication forks. We hence orient all chromosome configurations to break these symmetries (Methods). This orientation allows us to look for indicators of chromosome and fork segregation in the data.

Mean long-axis positions of monomers show that, without loop-extruders, for $N/4 \leq R < N$, the replication forks are on average in different cell halves (Fig. 2A). The replication forks are hence clearly separated along the long-axis of the cell, and the replicated chromosomal strands are mostly aligned in slightly shifted left-*ori*-right configurations. By contrast, with loop-extruders the chromosomes are in *ori-ori-ter* ($R < N/2$) or *ori-ter-ori* ($R > N/2$) configurations, as predicted by our segregation model. Furthermore, alignment of the chromosomal arms by loop-extruders implies that the replication forks coincide at roughly the same mean long-axis coordinate, consistent with experimental evidence that replication forks often colocalize in *C. crescentus* (36, 54) and other bacterial species (55).

The preferred chromosome orientations can also be seen from simulated contact maps, which measure how frequently two genomic regions are spatially close to each other. The cis-contact maps of chromosomes (Fig. 2C, Supplementary Fig. 6) without loop-extrusion show an off-diagonal line of enhanced contacts starting from mid-arm of the chromosome, indicative of a left-*ori*-right organization. With loop-extruders, by contrast, the off-diagonal line starts from the origin of replication, indicative of an *ori-ter* configuration.

We also find that trans-contact maps show less contacts between replicated chromosomal strands with loop-extruders than without (Fig. 2D, Supplementary Fig. 6), further illustrating how loop-extrusion enhances segregation.

To better understand fork segregation in the absence of loop-extruders, we analyze the mean long-axis separation between replication forks. We find that the fork separation can be qualitatively predicted by presuming that the polymer strands are all equally compressed along the long-axis of the cell (Supplementary Note 7, Fig. 2E). In the presence of loop-extruders, a similar argument can be used to predict the average long-axis separation between replication forks and the *ori* (Fig. 2F). Our findings indicate that, as replication progresses in the absence of loop-extruders, the forks approach each other as the unreplicated segment between them shrinks, so that there is a smooth transition from fork-segregated to chromosome-segregated states. With loop-extruders, on the other hand, we expect a smooth transition towards segregated states half-way through replication.

Since loop-extruders effectively bring the replication forks together, one can ask whether connecting the replication forks into a "replication factory" (4, 41, 55) would be sufficient to explain the enhancement of segregation we observe due to loop-extrusion. To test this hypothesis, we simulate steady-state configurations of a model where the replication forks are tied together in the absence of loop-extruders. We find that although the replication factory model shows better segregation than the model with neither loop-extruders nor a replication factory, segregation is still significantly better with only loop-extruders (Supplementary Note 8, Supplementary Fig. 11). Even if the replication forks are tied together, in the absence of loop-extruders, the two arms of a newly replicated strand can spread in opposite directions across the long axis of the cell. We hence find that the effective linearization of the origin proximal regions by loop-extruders, which prevents this arm spreading, is important for redirecting entropic forces towards segregation.

To quantify the long-axis segregation of the chromosomes using a simple metric, we calculate the segregated fraction: the fraction of replicated monomers in the correct cell half, minus the fraction in the incorrect cell half. For all simulated values of R, we find that the the segregated fraction at steady-state is larger in the presence of loop-extruders (Fig. 2G). To see whether purely entropic forces still lead to some segregation in the absence of loop-extruders, we compare the segregated fraction to values from simulations with an ideal polymer, where chains can freely mix because of the absence of excluded volume interactions (Fig. 2G). For $R \leq N/2$, the segregated fraction without loop-extruders is close to that of the ideal polymer, suggesting that entropic forces do not lead to significant segregation. Indeed, as predicted by our segregation model, it is only when we approach the limit of fully replicated chromosomes that entropic segregation without loop-extruders becomes significant, as reflected by the increase in the segregated fraction beyond the ideal polymer reference line. However, even in the limit of fully replicated chromosomes, the segregated fraction remains substantially higher with loop-extruders (mean 0.92, standard deviation 0.02) than without (mean 0.71, standard deviation 0.20). This improvement of segregation by loop-extruders could be due to repulsion between chromosomal loops (14) caused by off-target loop-extruder loading. Thus, although purely entropic forces drive segregation of fully replicated chromosomes, as previously predicted (4), loop-extruders drive segregation at earlier replication stages and additionally enhance the segregation of terminal regions (Fig. 2A, D), thus enabling stronger segregation right before cell division.

Together, these numerical results confirm our topo-entropic segregation model, showing that purely entropic forces push chromosomes towards fork-segregated left-*ori*-right configurations until late replication stages, and hence inhibit segregation. This is consistent with previous steady-state simulations where half-replicated chromosomes did not demix unless Macrodomain constraints were included (19). We find that topo-entropic forces directed by loop-extruders can drive chromosome segregation at earlier replication stages. Even when replication is nearly complete and purely entropic forces become segregative, topo-entropic forces still drive stronger segregation. These results suggest that loop-extrusion could significantly enhance segregation during a dynamic replication process.

Loop-extrusion drives robust simultaneous segregation and replication. Our simulations at fixed replication stages indicate the direction of (topo-)entropic forces on partially replicated chromosomes. However, it is unclear how these entropic forces affect the dynamics of rapidly replicating chromosomes. Next, we investigate whether chromosomes undergoing dynamic replication in growing cells, where the polymer does not have time to fully relax, will display similar global organization as in the converged steady-state simulations. Importantly, the time-scale of polymer relaxation in our dynamic simulations is set such that the diffusivity of the origin of replication matches experimental data (56) (Supplementary Note 9, Supplementary Fig. 9).

All simulations are initialized with a single chromosome in an *ori-ter* orientation. Animations from our simulations readily show that simulated replicating chromosomes do not segregate without loop-extruders (Fig. 3A, Supplementary Video 1). This contrasts previous work (4) where segregation during replication was achieved using the concentric-shell model. Our simulations with loop-extruders, on the other hand, show clear transitions to segregated states roughly half-way through replication (Fig. 3B, Supplementary Video 2). This difference is striking: we find that the segregated fraction in the absence of loop-extruders is worse than what is achieved by chance in an ideal chain for the first half of replication, and plateaus at roughly 0.2 , close to ideal chain values. By contrast, with loop extruders the segregated fraction reaches values of 0.7 (Fig. 3C). This indicates that, while purely entropic forces in dynamically replicating systems hardly contribute to the dynamic segregation of replicating chromosomes, topo-entropic forces enable rapid large-scale chromosome segregation.

Despite starting from an *ori-ter* configuration before repli-

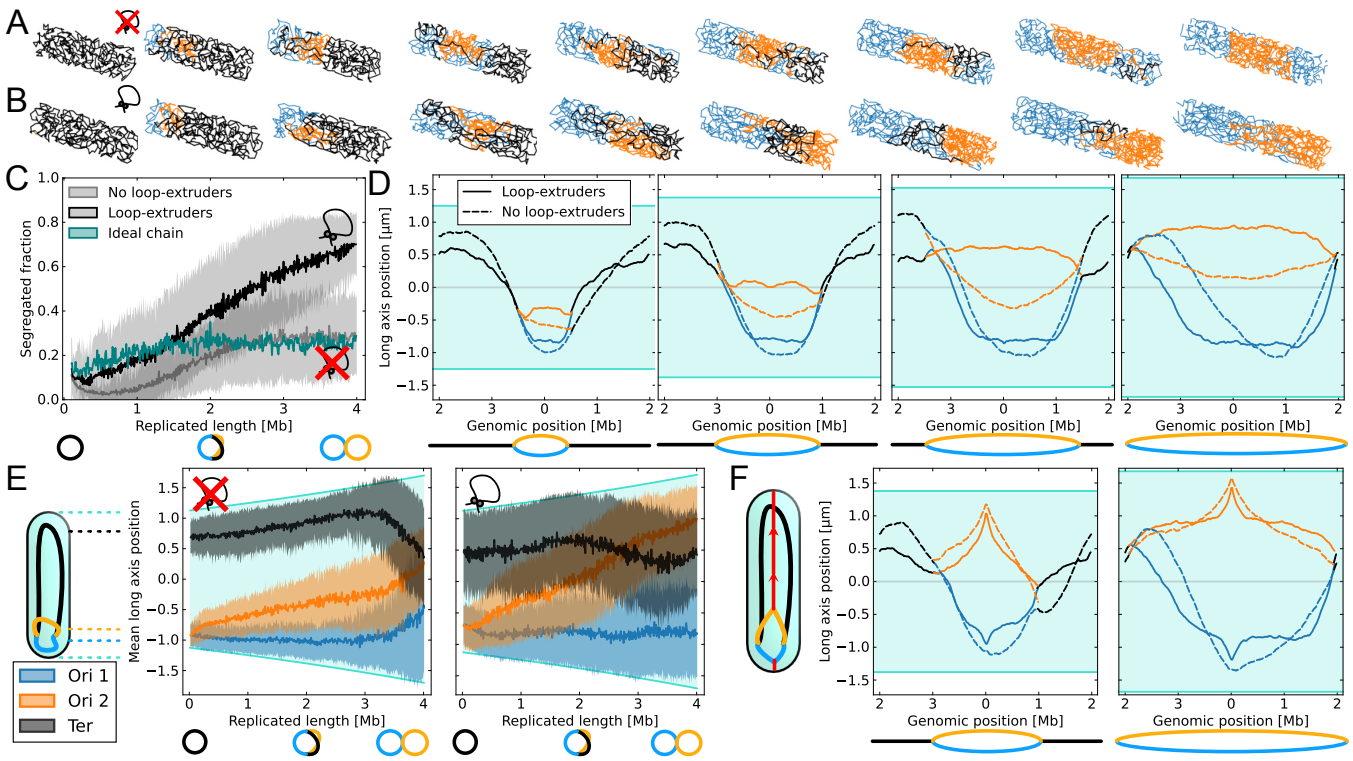

Fig. 3. Dynamic simulations of chromosome organization **A** Snapshots from simulations of a replicating chromosome without loop-extruders or *ori*-pulling forces, with replication progressing from left to right. Orange and blue lines are newly replicated chromosomal strands, the black line is the unreplicated strand. **B** Snapshots from simulations with loop-extruders but no *ori*-pulling forces. Roughly half-way through replication, the replicated strands start to segregate along the long-axis of the cell. **C** The segregated fraction as a function of replicated length during replication, from simulations with loop-extruders, without loop-extruders, and for an ideal chain without loop-extruders. For clarity, the standard deviation is only shown for simulations with excluded volume interactions, see Supplementary Fig. 8 for the standard deviation of the ideal chain simulations. **D** Mean long-axis positions of chromosomal regions as a function of genomic position from dynamic simulation at different replication stages (as in Fig. 2B). Despite starting from an *ori-ter* organization, without loop-extruders dynamic simulations exhibit fork segregation. Regions around the replication forks appear intermingled. With loop-extruders, segregation is more robust. **E** Mean long-axis position of genomic regions *ori* 1, *ori* 2, and *ter* across the replication cycle. Without loop-extruders, the origins of replication follow similar paths towards mid-cell, consistent with a transition towards a fork-segregated, left-*ori*-right organization. With loop-extruders, half-way through replication we observe the terminal region move towards mid-cell, indicating the predicted transition from an *ori-ori-ter* to an *ori-ter-ori* configuration. **F** Mean long-axis positions of chromosomal regions at $R = N/2$ and $R = N$, from simulations with origin-pulling forces. Fork segregation without loop-extruders is still visible for $R = N/2$. At the end of replication, terminal regions are better segregated with loop-extruders.

cation, chromosomes without loop-extruders start to rotate towards fork-segregated states during dynamic simulations, as can be confirmed from the average long-axis positions of monomers (Fig. 3D). With loop-extruders, on the other hand, the chromosomes maintain clear *ori-ter* configurations throughout the replication cycle. This suggests that loop-extrusion can allow replicating chromosomes to maintain their orientation.

Tracking the *ori*s and the *ter* over time reveals that, without loop-extruders, both origins of replication slowly move towards mid-cell, as expected for left-*ori*-right configurations (Fig. 3E). By contrast, in the presence of loop-extruders, the origins of replication separate at a steady rate as the genomic distance between them grows. The terminal region starts to move towards mid-cell when $R \approx N/2$, corresponding to the transition from an *ori-ori-ter* configuration to an *ori-ter-ori* configuration predicted by our segregation model.

Overall, our results show that even if replication proceeds rapidly compared to the relaxation of the chromosome, topo-entropic forces directed by loop-extruders drive effective chromosome segregation concurrent with replication, in line with our topo-entropic segregation model. To study how sensitively this result depends on our choice of parameters, we perform simulations with different numbers of loop-extruders (Supplementary Note 10, Supplementary Fig. 10) as well as faster loop-extruder off-loading (Supplementary Note 11, Supplementary Fig. 11). Faster off-loading implies that loop-extruders remain localized to narrower region around the origin, as seen in *C. crescentus* (49). Remarkably, we find that our central results are robust to varying these parameters over a broad range, indicating that loop-extruders can contribute to bacterial chromosome segregation even in smaller numbers, and even if they do not travel all the way from the origin to the terminus.

Loop-extruders complement origin segregation by separating terminal regions. To study how loop-extrusion can interact with a ParAB*S*-like mechanism, we include origin-pulling forces in our simulations. We find that in steady-state simulations without loop-extruders, fork segregation occurs even if *ori*-proximal regions are pulled to opposite poles of the cell (Fig. 2B, Supplementary Fig. 12). This result can be rationalized by noting that even if the origins of replication are tethered, fork segregation creates regions where fewer chromosomal strands overlap (Fig. 1A,B). Inclusion of loop-extruders prevents fork segregation, and

hence enhances sister chromosome segregation near the replication forks.

In dynamically replicating simulations, we find that early on in the replication process, pulling origins apart leads to faster segregation without loop-extruders, at a rate comparable to that of an ideal chain (Supplementary Fig. 12; Supplementary Videos S3, S4). Since loop-extruders compact and sometimes interlink the replicated strands, loop-extruders can also oppose the stretching of replicated chromosomal strands across the length of the cell at these early replication stages. However, at later replication stages, when entropy favors fork segregation via extension of the unreplicated strand, loop-extruders start to enhance segregation. This is also visible in the mean long-axis positions of the chromosomal regions (Fig. 3F): although most genomic regions are clearly segregated to opposite cell halves, *ter*-proximal regions are intermingled without loop-extrusion. We hence find that ParAB*S*-like forces alone can be sufficient to maintain chromosome orientation and to largely segregate bacterial chromosomes as may be expected, but they can be insufficient to efficiently segregate terminal regions. Interestingly, in the presence of loop-extruders, segregation is as accurate with or without origin-pulling in our simulations.

Discussion

In this work, we have developed a topo-entropic segregation model, which we confirmed with detailed simulations, to conceptually understand how distinct bacterial chromosome segregation mechanisms work in unison, when during the replication process they are effective, and whether they allow for global or local segregation (Fig. 4). Our model reveals that purely entropic forces cause partially replicated circular chromosomes to adopt unsegregated left-*ori*-right configurations. In accordance, our steady-state simulations without loop-extrusion did not exhibit segregation except at late replication stages, whereas our dynamic simulations revealed that purely entropic forces hardly contribute to chromosome segregation. Our findings contrast previous simulation results, where a concentric-shell model (4) or constraints on the replication forks (41) were used to achieve concurrent replication and segregation. Unlike these previous models, our work explains why dedicated mechanisms such as loop-extrusion or the ParAB*S* system are necessary to achieve concurrent chromosome replication and segregation: they are needed to overcome segregation-inhibiting entropic forces during replication. Finally, our topo-entropic segregation model elucidates how loop-extruders loaded at the origins of replication physically enhance segregation: the effective linearization of the origin-proximal regions turns segregation-inhibiting entropic forces into segregation-driving topo-entropic forces. Our simulations indicate that loop-extruders loaded at the origin can be sufficient to robustly drive global chromosome segregation.

Our simulation results further indicate that, whereas locally acting origin segregation forces are a good segregation mechanism at early replication stages, they do not lead to effective segregation of the terminal regions without loop-extruders.

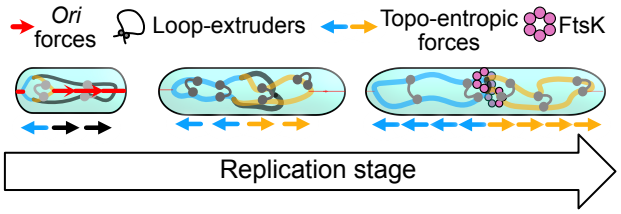

Fig. 4. Schematic model of the relative contributions of different bacterial chromosome segregation mechanisms. At initial replication states, *ori* segregation enables fast separation of newly replicated regions. Around half-way through replication, topo-entropic forces give the most important contribution. Finally, near the end stages of replication, purely entropic forces start to drive chromosome segregation, and factors such as loop-extrusion and FtsK help resolve terminal regions.

This suggests that ParAB*S*(-like) systems need to be complemented by other mechanisms, such as SMC-mediated topo-entropic forces, repulsion between SMC-loops (14), or terminus segregation mechanisms like FtsK. Thus our model can explain why simultaneously removing condensins and FtsK was found to be lethal in *B. subtilis* (40). Additionally, at late replication stages even purely entropic segregation forces become effective, especially if segregation has already been initiated (57, 58), suggesting that in species such as *C. crescentus*, origin segregation could be responsible for initiation, and entropic forces together with FtsK (essential in *C. crescentus* (25)) for completion of segregation. Loop-extrusion directed topo-entropic forces, by contrast, appear to facilitate chromosome segregation globally, and can be efficient even without origin segregation mechanisms, as observed in ParA-lacking mutants of *B. subtilis* (59).

Our work gives additional experimentally testable predictions: first, in the absence of loop-extruders loaded at the origin, replication fork separation should be observable; second, as the "ends" of effective linear segments, loop-extruder loading sites should be the first loci to segregate after replication; and third, in systems with sufficiently efficient loop-extrusion and an origin segregation system, loop-extrusion might be sufficient for chromosome segregation, whereas locally acting origin segregation forces should always be complemented by a mechanism for terminus segregation. Further work could also explore whether entropic fork segregation plays a role in establishing left-*ori*-right chromosome states in some bacteria, such as in *E. coli* (60) and transiently in *B. subtilis* (61).

Our work also provides insight into possible mechanisms of loop-extrusion in bacteria. In our model, we employed nontopological loop-extruders capable of by-passing obstacles (43, 62, 63), as opposed to topological loop-extruders that trap a chromosomal strand in a ring (64). When we repeated our simulations with topological loop-extruders, we found that chromosomal segregation was drastically inhibited (Supplementary Note 12, Supplementary Fig. 13). This suggests one possible reason why nontopological loop-extrusion might be preferred by bacteria.

The physical principles we have elucidated — on how entropy, specifically loaded loop-extruders, and locally acting forces act together to segregate and organize bacterial chromosomes — could be used to design segregation mechanisms

for synthetic cells (65) or "genomes-in-a-box" (66). Finally, although our work has focused on SMCs loaded at the origins of replication on an unstructured circular chromosome, our model for how topo-entropic forces orient polymers could be adapted to include structures such as Macrodomains (19) or CIDs (35), or for prokaryotic or eukaryotic systems with different patterns of loop-extruder loading.

Acknowledgments

We thank Cees Dekker, Bela Mulder and Tom Brandstätter for discussions, as well as Hugo Brandão and Leonid Mirny both for discussions and help with simulations.

Data and code availability

Simulation code can be accessed at github.com/PLSysGitHub/loop-extrusion_with_replication. Simulated data and the code used for analysis can be accessed at github.com/PLSysGitHub/loop-extrusion_with_replication_analysis.

Methods

Orienting sampled chromosome configurations. Since the two replicated strands and two arms on a partially replicated chromosome are indistinguishable, when averaging over many simulations, the mean positions of both replication forks and both *ori*s are equal. Hence, to distinguish whether chromosomes or replication forks segregate, each simulated configuration is oriented so that these symmetries are broken. We define Strand 1 such that the center of mass of Strand 1 and the unreplicated segment is closer to mid-cell than Strand 2 and the unreplicated segment (Supplementary Fig. 14A). Pole 1 is defined as the pole closer to Strand 1. Arm 1 is defined as the arm of Strand 1 and the unreplicated segment that is closer to Pole 1 (Supplementary Fig. 14B). When *ori*-pulling forces are simulated, the strands are not renamed, since the applied forces distinguish the two replicated strands.

In replicating simulations, the direction of replication distinguishes the terminal region. In steady-state simulations with loop-extruders, the terminal region lacks a loop-extruder loading site. However, in steady-state simulations without loop-extrusion, when $R = N/2$, all three chromosomal strands are indistinguishable. In this case, we label Strand 1 as the one with a center of mass closest to a pole, Strand 2 as the strand closest to mid-cell, and Strand 3 as the strand closest to the other pole.

1. Xindan Wang, Paula Montero Llopis, and David Z. Rudner. Organization and segregation of bacterial chromosomes. *Nat. Rev. Genet.*, 14:191–203, March 2013. ISSN 1471-0064. doi: 10.1038/nrg3375.
2. Anjana Badrinarayanan, Tung B. K. Le, and Michael T. Laub. Bacterial Chromosome Organization and Segregation. *Annu. Rev. Cell Dev. Biol.*, 31(1):171–199, November 2015. ISSN 1081-0706. doi: 10.1146/annurev-cellbio-100814-125211.
3. Christos Gogou, Aleksandre Japaridze, and Cees Dekker. Mechanisms for Chromosome Segregation in Bacteria. *Front. Microbiol.*, 12, June 2021. ISSN 1664-302X. doi: 10.3389/fmicb.2021.685687.
4. Suckjoon Jun and Bela Mulder. Entropy-driven spatial organization of highly confined polymers: Lessons for the bacterial chromosome. *Proc. Natl. Acad. Sci. U.S.A.*, 103(33):12388–12393, August 2006. doi: 10.1073/pnas.0605305103.
5. H. Niki, A. Jaffé, R. Imamura, T. Ogura, and S. Hiraga. The new gene mukB codes for a 177 kd protein with coiled-coil domains involved in chromosome partitioning of E. coli. *EMBO J.*, 10(1):183–193, January 1991. ISSN 1460-2075. doi: 10.1002/j.1460-2075.1991.tb07935.x.
6. P. L. Graumann. Bacillus subtilis SMC is required for proper arrangement of the chromosome and for efficient segregation of replication termini but not for bipolar movement of newly duplicated origin regions. *J. Bacteriol.*, 182(22):6463–6471, November 2000. ISSN 0021-9193. doi: 10.1128/JB.182.22.6463-6471.2000.
7. Stephan Gruber and Jeff Errington. Recruitment of Condensin to Replication Origin Regions by ParB/SpoOJ Promotes Chromosome Segregation in B. subtilis. *Cell*, 137(4):685–696, May 2009. ISSN 0092-8674. doi: 10.1016/j.cell.2009.02.035.
8. Xindan Wang, Hugo B. Brandão, Tung B. K. Le, Michael T. Laub, and David Z. Rudner. Bacillus subtilis SMC complexes juxtapose chromosome arms as they travel from origin to terminus. *Science*, 355(6324):524–527, February 2017. ISSN 0036-8075. doi: 10.1126/science.aai8982.
9. Daniel Chi-Hong Lin and Alan D. Grossman. Identification and Characterization of a Bacterial Chromosome Partitioning Site. *Cell*, 92(5):675–685, March 1998. ISSN 0092-8674. doi: 10.1016/S0092-8674(00)81135-6.
10. Dane A. Mohl, Jesse Easter, and James W. Gober. The chromosome partitioning protein, ParB, is required for cytokinesis in Caulobacter crescentus. *Mol. Microbiol.*, 42(3):741–755, November 2001. ISSN 0950-382X. doi: 10.1046/j.1365-2958.2001.02643.x.
11. Esteban Toro, Sun-Hae Hong, Harley H. McAdams, and Lucy Shapiro. Caulobacter requires a dedicated mechanism to initiate chromosome segregation. *Proc. Natl. Acad. Sci. U.S.A.*, 105(40):15435–15440, October 2008. doi: 10.1073/pnas.0807448105.
12. James M. Polson and Deanna R.-M. Kerry. Segregation of polymers under cylindrical confinement: effects of polymer topology and crowding. *Soft Matter*, 14(30):6360–6373, August 2018. ISSN 1744-683X. doi: 10.1039/C8SM01062E.
13. James M. Polson and Qinxin Zhu. Free energy and segregation dynamics of two channel-confined polymers of different lengths. *Phys. Rev. E*, 103(1):012501, January 2021. doi: 10.1103/PhysRevE.103.012501.
14. Anton Goloborodko, Maxim V. Imakaev, John F. Marko, and Leonid Mirny. Compaction and segregation of sister chromatids via active loop extrusion. *eLife*, May 2016. doi: 10.7554/eLife.14864.
15. Debarshi Mitra, Shreerang Pande, and Apratim Chatterji. Polymer architecture orchestrates the segregation and spatial organization of replicating E. coli chromosomes in slow growth. *Soft Matter*, 18(30):5615–5631, August 2022. ISSN 1744-683X. doi: 10.1039/D2SM00734G.
16. Suckjoon Jun and Andrew Wright. Entropy as the driver of chromosome segregation. *Nat. Rev. Microbiol.*, 8(8):600–607, August 2010. ISSN 1740-1534. doi: 10.1038/nrmicro2391.
17. Chris D. Webb, Aurelio Teleman, Scott Gordon, Aaron Straight, Andrew Belmont, Daniel Chi-Hong Lin, Alan D. Grossman, Andrew Wright, and Richard Losick. Bipolar Localization of the Replication Origin Regions of Chromosomes in Vegetative and Sporulating Cells of B. subtilis. *Cell*, 88(5):667–674, March 1997. ISSN 0092-8674. doi: 10.1016/S0092-8674(00)81909-1.
18. Patrick H. Viollier, Martin Thanbichler, Patrick T. McGrath, Lisandra West, Maliwan Meewan, Harley H. McAdams, and Lucy Shapiro. Rapid and sequential movement of individual chromosomal loci to specific subcellular locations during bacterial DNA replication. *Proc. Natl. Acad. Sci. U.S.A.*, 101(25):9257–9262, June 2004. doi: 10.1073/pnas.0402606101.
19. Ivan Junier, Frédéric Boccard, and Olivier Espéli. Polymer modeling of the E. coli genome reveals the involvement of locus positioning and macrodomain structuring for the control of chromosome conformation and segregation. *Nucleic Acids Res.*, 42(3):1461–1473, February 2014. ISSN 0305-1048. doi: 10.1093/nar/gkt1005.
20. Sophie Nolivos and David Sherratt. The bacterial chromosome: architecture and action of bacterial SMC and SMC-like complexes. *FEMS Microbiol. Rev.*, 38(3):380–392, May 2014. ISSN 0168-6445. doi: 10.1111/1574-6976.12045.
21. Stephan Gruber, Jan-Willem Veening, Juri Bach, Martin Blettinger, Marc Bramkamp, and Jeff Errington. Interlinked Sister Chromosomes Arise in the Absence of Condensin during Fast Replication in B. subtilis. *Curr. Biol.*, 24(3):293–298, February 2014. ISSN 0960-9822. doi: 10.1016/j.cub.2013.12.049.
22. Xuan-Chuan Yu, Elizabeth K. Weihe, and William Margolin. Role of the C Terminus of FtsK in Escherichia coli Chromosome Segregation. *J. Bacteriol.*, December 1998. doi: 10.1128/jb.180.23.6424-6428.1998.
23. Ling Juan Wu and Jeffery Errington. Bacillus subtilis spoIIIE Protein Required for DNA Segregation During Asymmetric Cell Division. *Science*, 264(5158):572–575, April 1994. ISSN 0036-8075. doi: 10.1126/science.8160014.
24. M. E. Sharpe and J. Errington. Postseptational chromosome partitioning in bacteria. *Proc. Natl. Acad. Sci. U.S.A.*, 92(19):8630, September 1995. doi: 10.1073/pnas.92.19.8630.
25. Sherry C. E. Wang, Lisandra West, and Lucy Shapiro. The Bifunctional FtsK Protein Mediates Chromosome Partitioning and Cell Division in Caulobacter. *J. Bacteriol.*, February 2006.
26. Adam S. B. Jalal and Tung B. K. Le. Bacterial chromosome segregation by the ParABS system. *Open Biol.*, 10(6):200097, June 2020. ISSN 2046-2441. doi: 10.1098/rsob.200097.
27. Sarah Bigot, Viknesh Sivanathan, Christophe Possoz, François-Xavier Barre, and François Cornet. FtsK, a literate chromosome segregation machine. *Mol. Microbiol.*, 64(6):1434–1441, June 2007. ISSN 0950-382X. doi: 10.1111/j.1365-2958.2007.05755.x.
28. Mathieu Stouf, Jean-Christophe Meile, and François Cornet. FtsK actively segregates sister chromosomes in Escherichia coli. *Proc. Natl. Acad. Sci. U.S.A.*, 110(27):11157–11162, July 2013. doi: 10.1073/pnas.1304080110.
29. Conrad W. Shebelut, Jonathan M. Guberman, Sven van Teeffelen, Anastasiya A. Yakhnina, and Zemer Gitai. Caulobacter chromosome segregation is an ordered multistep process. *Proc. Natl. Acad. Sci. U.S.A.*, 107(32):14194–14198, August 2010. doi: 10.1073/pnas.1005274107.
30. Hoong Chuin Lim, Ivan Vladimirovich Surovtsev, Bruno Gabriel Beltran, Fang Huang, Jörg Bewersdorf, and Christine Jacobs-Wagner. Evidence for a DNA-relay mechanism in ParABS-mediated chromosome segregation. *eLife*, May 2014. doi: 10.7554/eLife.02758.
31. Ivan V. Surovtsev, Manuel Campos, and Christine Jacobs-Wagner. DNA-relay mechanism is sufficient to explain ParA-dependent intracellular transport and patterning of single and

multiple cargos. *Proc. Natl. Acad. Sci. U.S.A.*, 113(46):E7268–E7276, November 2016. doi: 10.1073/pnas.1616118113.

32. J.-C. Walter, J. Dorignac, V. Lorman, J. Rech, J.-Y. Bouet, M. Nollmann, J. Palmeri, A. Parmeggiani, and F. Geniet. Surfing on Protein Waves: Proteophoresis as a Mechanism for Bacterial Genome Partitioning. *Phys. Rev. Lett.*, 119(2):028101, July 2017. ISSN 1079-7114. doi: 10.1103/PhysRevLett.119.028101.
33. Christian Hanauer, Silke Bergeler, Erwin Frey, and Chase P. Broedersz. Theory of Active Intracellular Transport by DNA Relaying. *Phys. Rev. Lett.*, 127(13):138101, September 2021. ISSN 1079-7114. doi: 10.1103/PhysRevLett.127.138101.
34. Monica A. Schwartz and Lucy Shapiro. An SMC ATPase mutant disrupts chromosome segregation in Caulobacter. *Mol. Microbiol.*, 82(6):1359–1374, December 2011. ISSN 0950-382X. doi: 10.1111/j.1365-2958.2011.07836.x.
35. Tung B.K. Le, Maxim V. Imakaev, Leonid A. Mirny, and Michael T. Laub. High-resolution mapping of the spatial organization of a bacterial chromosome. *Science*, 342(6159):731–734, 2013. ISSN 10959203. doi: 10.1126/science.1242059.
36. Rodrigo Arias-Cartin, Genevieve S. Dobihal, Manuel Campos, Ivan V. Surovtsev, Bradley Parry, and Christine Jacobs-Wagner. Replication fork passage drives asymmetric dynamics of a critical nucleoid-associated protein in Caulobacter. *EMBO J.*, 36(3):301–318, February 2017. ISSN 1460-2075. doi: 10.15252/embj.201695513.
37. S. Hiraga, H. Niki, R. Imamura, T. Ogura, K. Yamanaka, J. Feng, B. Ezaki, and A. Jaffé. Mutants defective in chromosome partitioning in E. coli. *Res. Microbiol.*, 142(2):189–194, January 1991. ISSN 0923-2508. doi: 10.1016/0923-2508(91)90029-A.
38. Philina S. Lee and Alan D. Grossman. The chromosome partitioning proteins Soj (ParA) and Spo0J (ParB) contribute to accurate chromosome partitioning, separation of replicated sister origins, and regulation of replication initiation in Bacillus subtilis. *Mol. Microbiol.*, 60 (4):853–869, May 2006. ISSN 0950-382X. doi: 10.1111/j.1365-2958.2006.05140.x.
39. Xindan Wang, Olive W. Tang, Eammon P. Riley, and David Z. Rudner. The SMC Condensin Complex Is Required for Origin Segregation in Bacillus subtilis. *Curr. Biol.*, 24(3):287–292, February 2014. ISSN 0960-9822. doi: 10.1016/j.cub.2013.11.050.
40. R. A. Britton and A. D. Grossman. Synthetic lethal phenotypes caused by mutations affecting chromosome partitioning in Bacillus subtilis. *J. Bacteriol.*, 181(18):5860–5864, September 1999. ISSN 0021-9193. doi: 10.1128/JB.181.18.5860-5864.1999.
41. N. El Najjar, D. Geisel, F. Schmidt, S. Dersch, B. Mayer, R. Hartmann, B. Eckhardt, P. Lenz, and Graumann P. L. Chromosome Segregation in Bacillus subtilis Follows an Overall Pattern of Linear Movement and Is Highly Robust against Cell Cycle Perturbations. *mSphere*, 5(3): e00255–20, June 2020. ISSN 2379-5042. doi: 10.1128/msphere.00255-20.
42. Hugo B Brandão, Payel Paul, Aafke A van den Berg, David Z Rudner, Xindan Wang, and Leonid A Mirny. Rna polymerases as moving barriers to condensin loop extrusion. *Proceedings of the National Academy of Sciences*, 116(41):20489–20499, 2019.
43. Hugo B. Brandão, Zhongqing Ren, Xheni Karaboja, Leonid A. Mirny, and Xindan Wang. DNA-loop-extruding SMC complexes can traverse one another in vivo. *Nat. Struct. Mol. Biol.*, 28(8):642–651, Aug 2021. ISSN 1545-9985. doi: 10.1038/s41594-021-00626-1.
44. Ruth Kavenoff and Oliver A. Ryder. Electron microscopy of membrane-associated folded chromosomes of Escherichia coli. *Chromosoma*, 55(1):13–25, March 1976. ISSN 1432-0886. doi: 10.1007/BF00288323.
45. James Pelletier, Ken Halvorsen, Bae-Yeun Ha, Raffaella Paparcone, Steven J. Sandler, Conrad L. Woldringh, Wesley P. Wong, and Suckjoon Jun. Physical manipulation of the Escherichia coli chromosome reveals its soft nature. *Proc. Natl. Acad. Sci. U.S.A.*, 109(40): E2649–E2656, October 2012. doi: 10.1073/pnas.1208689109.
46. Fabai Wu, Aleksandre Japaridze, Xuan Zheng, Jakub Wiktor, Jacob W. J. Kerssemakers, and Cees Dekker. Direct imaging of the circular chromosome in a live bacterium. *Nat. Commun.*, 10(2194):1–9, May 2019. ISSN 2041-1723. doi: 10.1038/s41467-019-10221-0.
47. Larissa Wilhelm, Frank Bürmann, Anita Minnen, Ho-Chul Shin, Christopher P. Toseland, Byung-Ha Oh, and Stephan Gruber. SMC condensin entraps chromosomal DNA by an ATP hydrolysis dependent loading mechanism in Bacillus subtilis. *eLife*, May 2015. doi: 10.7554/eLife.06659.
48. Anita Minnen, Laetitia Attaiech, Maria Thon, Stephan Gruber, and Jan-Willem Veening. SMC is recruited to oriC by ParB and promotes chromosome segregation in Streptococcus pneumoniae. *Mol. Microbiol.*, 81(3):676–688, August 2011. ISSN 0950-382X. doi: 10.1111/j.1365-2958.2011.07722.x.
49. Ngat T. Tran, Michael T. Laub, and Tung B. K. Le. SMC Progressively Aligns Chromosomal Arms in Caulobacter crescentus but Is Antagonized by Convergent Transcription. *Cell Rep.*, 20(9):2057–2071, August 2017. ISSN 2211-1247. doi: 10.1016/j.celrep.2017.08.026.
50. Jeffrey M. Skerker and Michael T. Laub. Cell-cycle progression and the generation of asymmetry in Caulobacter crescentus. *Nat. Rev. Microbiol.*, 2(4):325–337, April 2004. ISSN 1740-1526. doi: 10.1038/nrmicro864.
51. Dan Siegal-Gaskins and Sean Crosson. Tightly regulated and heritable division control in single bacterial cells. *Biophys. J.*, 95(4):2063–2072, August 2008. ISSN 1542-0086. doi: 10.1529/biophysj.108.128785.
52. Joris J. B. Messelink, Muriel C. F. van Teeseling, Jacqueline Janssen, Martin Thanbichler, and Chase P. Broedersz. Learning the distribution of single-cell chromosome conformations in bacteria reveals emergent order across genomic scales. *Nat. Commun.*, 12(1963):1–9, March 2021. ISSN 2041-1723. doi: 10.1038/s41467-021-22189-x.
53. Janni Harju, Joris J. B. Messelink, Grzegorz Gradziuk, Muriel C. F. van Teeseling, and Chase P. Broedersz. In preparation, 2023. Data on separation between origins of replication over the cell cycle.
54. Rasmus B. Jensen, Sherry C. Wang, and Lucy Shapiro. A moving DNA replication factory in Caulobacter crescentus. *EMBO J.*, 20(17):4952–4963, September 2001. ISSN 1460-2075. doi: 10.1093/emboj/20.17.4952.
55. Sarah M. Mangiameli, Brian T. Veit, Houra Merrikh, and Paul A. Wiggins. The Replisomes Remain Spatially Proximal throughout the Cell Cycle in Bacteria. *PLos Genet.*, 13(1): e1006582., January 2017. ISSN 1553-7404. doi: 10.1371/journal.pgen.1006582.
56. Stephanie C. Weber, Andrew J. Spakowitz, and Julie A. Theriot. Nonthermal ATP-dependent fluctuations contribute to the in vivo motion of chromosomal loci. *Proc. Natl. Acad. Sci. U.S.A.*, 109(19):7338–7343, May 2012. doi: 10.1073/pnas.1119505109.
57. Elena Minina and Axel Arnold. Induction of entropic segregation: the first step is the hardest. *Soft Matter*, 10(31):5836–5841, 2014. doi: 10.1039/C4SM00286E.
58. Elena Minina and Axel Arnold. Entropic Segregation of Ring Polymers in Cylindrical Confinement. *Macromolecules*, 48(14):4998–5005, July 2015. ISSN 0024-9297. doi: 10.1021/acs.macromol.5b00636.
59. K. Ireton, Gunther N. W. 4th, and Grossman A. D. spo0J is required for normal chromosome segregation as well as the initiation of sporulation in Bacillus subtilis. *J. Bacteriol.*, 176(17): 5320–5329, September 1994. ISSN 0021-9193. doi: 10.1128/jb.176.17.5320-5329.1994.
60. Henrik J. Nielsen, Jesper R. Ottesen, Brenda Youngren, Stuart J. Austin, and Flemming G. Hansen. The Escherichia coli chromosome is organized with the left and right chromosome arms in separate cell halves. *Mol. Microbiol.*, 62(2):331–338, October 2006. ISSN 0950-382X. doi: 10.1111/j.1365-2958.2006.05346.x.
61. Xindan Wang, Paula Montero Llopis, and David Z. Rudner. Bacillus subtilis chromosome organization oscillates between two distinct patterns. *Proc. Natl. Acad. Sci. U.S.A.*, 111(35): 12877–12882, September 2014. doi: 10.1073/pnas.1407461111.
62. Eugene Kim, Jacob Kerssemakers, Indra A. Shaltiel, Christian H. Haering, and Cees Dekker. DNA-loop extruding condensin complexes can traverse one another. *Nature*, 579 (7799):438–442, March 2020. ISSN 1476-4687. doi: 10.1038/s41586-020-2067-5.
63. Biswajit Pradhan, Roman Barth, Eugene Kim, Iain F. Davidson, Benedikt Bauer, Theo van Laar, Wayne Yang, Je-Kyung Ryu, Jaco van der Torre, Jan-Michael Peters, and Cees Dekker. SMC complexes can traverse physical roadblocks bigger than their ring size. *Cell Rep.*, 41(3):111491, October 2022. ISSN 2211-1247. doi: 10.1016/j.celrep.2022.111491.
64. Kirill Polovnikov and Bogdan Slavov. Topological and nontopological mechanisms of loop formation in chromosomes: Effects on the contact probability. *Phys. Rev. E*, 107(5):054135, May 2023. ISSN 2470-0053. doi: 10.1103/PhysRevE.107.054135.
65. Lorenzo Olivi, Mareike Berger, Ramon N. P. Creyghton, Nicola De Franceschi, Cees Dekker, Bela M. Mulder, Nico J. Claassens, Pieter Rein Ten Wolde, and John van der Oost. Towards a synthetic cell cycle. *Nat. Commun.*, 12(4531):1–11, July 2021. ISSN 2041-1723. doi: 10.1038/s41467-021-24772-8.
66. Anthony Birnie and Cees Dekker. Genome-in-a-Box: Building a Chromosome from the Bottom Up. *ACS Nano*, 15(1):111–124, January 2021. ISSN 1936-0851. doi: 10.1021/acsnano.0c07397.